Paleobiology, 27(1), 2001, pp. 104–125

Pleistocene adaptive radiation in *Globorotalia truncatulinoides*: genetic, morphologic, and environmental evidence

Colomban de Vargas, Sabrina Renaud, Heinz Hilbrecht, and Jan Pawlowski

Abstract.—*Globorotalia truncatulinoides* is an extant species of planktic foraminiferans commonly used for stratigraphic and paleoenvironmental analyses. It originated ~2.8 m.y. ago in subtropical areas of the South Pacific, spread to all subtropical and temperate regions of the world ocean, and expanded its range to southern subantarctic waters between 500 and 200 Ka. The wide geographic distribution of *G. truncatulinoides* is associated with a latitudinal morphological variability considered as an ecophenotypic variation within a single species. Here, we present the first molecular, morphological, and ecological evidence that *G. truncatulinoides* corresponds to a complex of four genetic species adapted to particular hydrographic conditions. The different species are separated by significant genetic distances in several ribosomal genes (SSU, ITS-1, 5.8S, ITS-2). Species 1 and species 2 characterize subtropical waters, species 3 is abundant exclusively in the Subantarctic Convergence, while species 4 inhabits subantarctic waters. By using an absolute molecular clock, we deduce the time of divergence between the subtropical and frontal/subantarctic species at ~300 Ka, which is in agreement with stratigraphic data and suggests an adaptive radiation of the species allowing it to colonize the nutrient-rich and cold subantarctic waters. This genetic dichotomy is associated with a morphological differentiation identified using outline analysis. Species of the same regions are more similar in test shape but can be distinguished by coiling direction. The evolutionary patterns recognized here by combining DNA and morphological analyses from plankton-tow specimens mirror and allow a new interpretation of the data available from Recent sediments. They highlight the importance of adaptation and heterochronic processes, leading to cryptic speciation, in planktic foraminifera.

Colomban de Vargas and Jan Pawlowski. Département de Zoologie et Biologie Animale, Université de Genève, CH-1224 Chêne-Bougeries, Switzerland*
Sabrina Renaud† and Heinz Hilbrecht. Geological Institute, ETH, CH-8092 Zürich, Switzerland
* Present address: *Department of Organismic and Evolutionary Biology (OEB), Harvard University, 16 Divinity Avenue, Cambridge, Massachusetts 02138. E-mail: cvargas@oeb.harvard.edu*
† Present address: *FRE 2158 CNRS, UCB Lyon I, F-69622 Villeurbanne, France*

Accepted: 24 July 2000

Introduction

The fossil record of deep-sea microfossils such as planktic foraminifera is exceptionally continuous in time and space, and therefore offers a unique opportunity for understanding processes of evolution and paleoceanography on a global scale.

Nevertheless, species concepts in planktic foraminifera are still very uncertain mostly because current taxonomy is based entirely on morphological criteria of the test (shell). Morphological taxonomy is an especially complex problem in these organisms because (1) the morphological characters of their tests are relatively few and (2) in most known morphotypes the variability of the few available morphocharacters is high across large geographic ranges. Although the biological meaning of morphological characters and their variability is a subject of debate, micropaleontologists generally cluster similar morphotypes into single species that commonly have a bipolar or even cosmopolitan biogeographic distribution. The resulting, relatively large intraspecific morphological variability of planktonic foraminifera is usually attributed to ecophenotypic or clinal variations. This may be one reason that the number of about 50 living species (Hemleben et al. 1989) is small in comparison with other plankton groups.

In fact, slight morphological differences may separate species of planktic foraminifera. Recent studies based on ribosomal DNA sequence analyses demonstrated the existence of cryptic species within all of the spinose planktic foraminifera analyzed (Huber et al. 1997; de Vargas et al. 1999; Darling et al. 1999). In the case of *Orbulina universa*, the genetic analysis of hundreds of specimens collected across

 0094-8373/01/2701-0008/$1.00

the Atlantic Ocean showed a patchy and alternating distribution of three genetically distinct species adapted to particular ranges of ocean surface productivity (de Vargas et al. 1999). This case raises the possibility that morphology-based species of planktic foraminifera may include several cryptic genetic species with much narrower ecological requirements and geographic ranges than the current morphological species concepts would suggest.

Using a biological—or at least genetic—concept of species could therefore allow us to refine our understanding of evolutionary processes, ecology and environmental preferences of planktic foraminifera. In this purpose, it is necessary to test if genetic speciation actually occurred in most morphologically defined species, to establish the ecological characteristics of the cryptic genetic species, and to estimate the synchronization between genetic and morphological differentiation.

The main objective of this study is to use molecular data to reconsider the morphological variability and biogeography of a well-known species of planktic foraminifer, *Globorotalia truncatulinoides*. We sequenced four different genes of the ribosomal cluster from more than 100 individuals of *G. truncatulinoides*, collected mostly between 15° and 50°S during the Atlantic Meridional Transect (AMT) cruise 5 (Robins and Aiken 1996). By analyzing the nucleotide substitutions between homologous DNA sequences, we have (1) differentiated the specimens into genetic entities (genotypes), (2) assessed the presence or absence of gene flow between the genotypes and thus the degree of their genetic isolation (populations or full species), (3) reconstructed the phylogeny of these genotypes, and (4) estimated the timing of the separation events using the molecular clock. Additionally, we applied a simple method of genetic identification to analyze the geographic distribution of the genotypes along the AMT transect from subtropical to polar waters. Morphometric analyses on populations from the same plankton tows were also performed to compare genetic and morphological patterns of differentiation in *G. truncatulinoides*. Finally, our results have been interpreted in an evolutionary perspective by comparing our morphogenetic results with paleontological data from Recent and Pleistocene sediments.

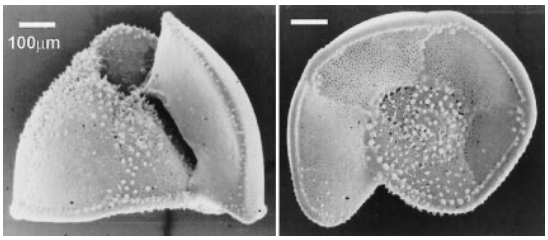

FIGURE 1. Morphology of *Globorotalia truncatulinoides*, a non-spinose globorotaliid planktic foraminifer. Left-coiled specimen from Bermuda.

Globorotalia truncatulinoides

Globorotalia truncatulinoides has a conical test with five ventrally elongated chambers in the final whorl and a keel along the entire periphery in adult specimens (Fig. 1). The spiral of the test may coil in a clockwise (right-coiling) or counterclockwise (left-coiling) direction. This species originated between 2.8 and 2.3 Ma in subtropical areas of the South Pacific as a descendant from *G. crassaformis* (Hills and Thierstein 1989; Lazarus et al. 1995). Its morphology diversified and significant phyletic change occurred in the Pacific for 600 k.y. after speciation. The species subsequently immigrated into the Indian and Atlantic Oceans between 2.3 and 1.9 Ma (Spencer-Cervato and Thierstein 1997). The history of *G. truncatulinoides* is then characterized by various regional morphological trends, such as the reversal in phyletic direction that produced populations morphologically similar to ancestral populations between 1.8 and 1.5 Ma (Lazarus et al. 1995), or the rapidly changing coiling direction characteristic of the North Atlantic record during the glacial/interglacial fluctuations (Spencer-Cervato and Thierstein 1997).

Limited to tropical and subtropical environments during the major part of its evolution, *G. truncatulinoides* has relatively recently colonized subpolar waters in the Southern Ocean. The first expansion of range to northern subantarctic waters happened at ~500 Ka (Pharr and Williams 1987). Since ~300 Ka, the species has occurred there permanently and it further expanded to southern subantarctic waters at ~200 Ka (Kennett 1970). The forms

that invaded high-latitude waters are smaller in size and possess a rounded, low-spired test morphology reminiscent of their putative ancestor, *G. crassaformis.*

The modern biogeography of *G. truncatulinoides* is well known from surface-sediment samples (Kennett 1968; Healy-Williams and Williams 1981; Healy-Williams 1983; Healy-Williams et al. 1985; Pharr and Williams 1987; Lohmann and Malmgren 1983; Lohmann and Schweitzer 1990; Lohmann 1992; Martinez 1997). This species is restricted to subtropical and tropical waters in the Northern Hemisphere but extends into subantarctic waters in the Southern Hemisphere (Kennett 1968). Its morphology varies with latitude from highly conical forms in tropical areas to compressed and convex forms in cold water of the Southern Ocean (Kennett 1968). Given the apparent absence of any morphological breaks within the species range, Kennett (1968) assigned this variation to an ecophenotypic cline related to a continuous response to surface-water temperature. Healy-Williams and coworkers (Healy-Williams and Williams 1981; Healy-Williams 1983; Healy-Williams et al. 1985) applied Fourier analyses on large samples from the southern Indian Ocean. They suggested the presence of a complex stepwise latitudinal shape variation due to mixing in various proportions of three morphotypes of *G. truncatulinoides*, each with distinct shell shape and isotopic composition.

Finally, detailed studies on modern *G. truncatulinoides* ecology from near Bermuda suggest that *G. truncatulinoides* lives and grows over a wide depth range, from the surface mixed layer to over 800 m depth, and is thought to reproduce on an annual basis during winter (Deuser et al. 1981; Hemleben et al. 1985; Lohmann and Schweitzer 1990). Fairbanks and Wiebe (1980) and Mulitza et al. (1997) concluded it is preferentially a deep-dwelling species calcifying its shell at the top of the thermocline. Lohmann and Schweitzer (1990) observed a relation between the size frequency distribution of the tests and the structure of the thermocline in plankton and surface-sediment samples. They proposed that vertical mixing down to the permanent thermocline (~600 m depth) is required for *G. truncatulinoides* to complete its full reproductive cycle.

Material

Plankton samples (Table 1) were collected with net tows (100-μm and 200-μm mesh size) between 200 m depth and the sea surface. *Globorotalia truncatulinoides* was found in 11 out of the 30 AMT stations sampled along a 50°N–50°S Atlantic transect in 1997 (see Fig. 9). Material from two additional stations sampled in 1996 was integrated into this study, the Med-Sea and Sargasso-Sea stations (Table 1) located offshore Villefranche-sur-Mer (France) and Bermuda, respectively. Conductivity temperature and depth (CTD) casts provided water temperature, salinity, fluorescence and transmissivity profiles at every 2 m between the sea surface and deep waters at each AMT station (except AMT-23, because of technical problems). The shipboard logger recorded temperature, salinity, and chlorophyll-a fluorescence at the sea surface (7 m depth) every 10′ along the entire AMT-5 transect; these data were used to distinguish surface water masses on a fine scale.

Methods

DNA Extraction.—Immediately after collection, specimens of *G. truncatulinoides* were sorted with a dissecting microscope, isolated, cleaned by brushing, and transferred to filtered sea water in petri dishes. A total of 142 DNA-extractions from individual cells were performed on the day of collection as described by de Vargas et al. (1997). Coiling direction of the tests was recorded prior to the destructive extraction procedure. Material from additional plankton tows at each AMT station was conserved in formalin for morphometric analyses. For a few specimens, we experimented with a new nondestructive method of DNA-extraction allowing us to obtain both the test and the DNA from single cells for further morphologic and genetic comparison.

Polymerase Chain Reaction (PCR) Amplification, Cloning, and Sequencing.—The genomic areas sequenced for the phylogenetic analyses are part of the gene coding for the small subunit of the ribosome (SSU rDNA) and for the

TABLE 1. Sampling sites with their corresponding: location, date, sample size for genetic, morphometric and morphogenetic analyses, environmental parameters at the sea surface and oceanographic provinces as defined by Hooker and Rees (in press) on several AMT cruises. SATG = South Atlantic Tropical Gyre province (15–31°S); BraC = Brazil Current province (31–35°S); SASh = South American Shelf province (35–40°); SanC = Sub-Antarctic Convergence province (40–46°S); FalC = Falkland Current province (46–50°S).

				Number of individual *G. truncatulinoides* analyzed for			Sea surface			
Station	Latitude	Longitude	Date	Genetics	Morphometrics	Morphogenetics*	Temp. (°C)	Salinity (‰)	Chyll. (ng/l)	Oceanic province
Med-Sea	43°40′N	07°15′E	4–18 Dec.	12	—		—	—	—	
Sargasso-Sea	32°20′N	64°33′W	9–25 Apr.	7	9		—	—	—	
AMT-8	32°19′N	17°14′W	25 Sept.	1	—		24.1	36.9	48.64	
AMT-19	16°41′S	32°22′W	7 Oct.	7	—		25.5	37.2	56.05	SATG
AMT-20	20°40′S	34°14′W	8 Oct.	10	4		23.9	37.1	80.68	SATG
AMT-21	23°54′S	37°17′W	9 Oct.	4	2	2	22.8	36.8	91.7	SATG
AMT-22	27°41′S	40°59′W	10 Oct.	14	1		20.9	36.6	183.6	SATG
AMT-23	31°37′S	44°52′W	11 Oct.	16	12	4	18.1	36.1	485.7	BraC
AMT-24	35°29′S	48°52′W	12 Oct.	2	2		18.7	35.8	271.5	SASh
AMT-25	38°50′S	51°55′W	13 Oct.	18	27		14.3	35.5	854.64	SAnC
AMT-26	42°14′S	54°27′W	14 Oct.	22	104		12.2	35.1	961.02	SAnC
AMT-28	46°03′S	56°42′W	15 Oct.	5	36		7.8	34.1	407.66	FalC
AMT-30	49°48′S	57°40′W	16 Oct.	—	5		5.6	33.9	376.33	FalC

* For those cells, a new method of DNA extraction without shell destruction allowed us to perform both genetic and morphologic analyses on the same individual.

internal transcribed spacers (ITS) region containing the ITS-1, ITS-2, and 5.8S ribosomal genes (Fig. 2). The PCR amplification, PCR product purification, and cloning of the ~1100-bp (base pairs) SSUr DNA fragment, as well as the foraminiferal specific primers, are described elsewhere (de Vargas et al. 1997). The ITS region is analyzed here for the first time in planktic foraminifera. To avoid contamination by exogenous genetic material, we designed new globorotaliid-specific primers. The primers *S30f* (5′ AAGAGAAGTCGTAA-

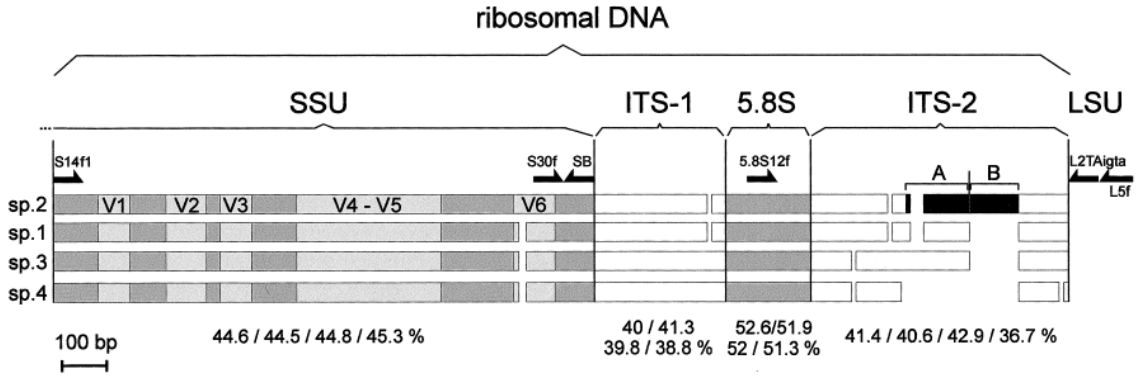

FIGURE 2. Diagram of the organization and respective length of the SSU, ITS-1, 5.8S and ITS-2 ribosomal genes of the four different *Globorotalia truncatulinoides* genotypes (sp. 1, sp. 2, sp. 3, and sp. 4). As in other Eukaryotes, the four genes are juxtaposed, forming a cluster that is repeated in a long array. Dark gray, gray, and white rectangles mark conservative, variable (V), and highly variable regions of the cluster. Deletions higher than 10 bp are indicated by interruptions in each cluster. A repeated unit of 104 bp present only in sp. 2 is represented by two black rectangles, A and B. The location of the primers used for PCR amplification and the analyzed fragments are shown above the sp. 2 cluster. Below are noted the G+C contents of each ribosomal region (given as sp. 1/sp. 2/sp. 3/sp. 4).

CAAGGC 3′)—*L5f* (5′ TCGCCGTTACTAAGGRAATC 3′) and *S30f*—*L2TAigta* (5′ GCGTAYCCTTRCCTGAGCT 3′) were used to amplify the whole ITS region at once with a standard PCR program: 94°C/30′-50°C/30′-72°/2′′ repeated 40 times. The primers *5.8S12f* (5′ GAATTGCAAGWCACATTGGC 3′), together with *L5f* or *L2TAigta*, were used for amplifying the ITS-2 gene alone. The amplified PCR products were then purified using the *High Pure PCR Purification* kit (Roche), ligated into the *pGEM-T Vector System* (Promega), cloned in the *XL-2 Ultracompetent Cells* (Stratagene), and sequenced with *ABI PRISM Big Dye Terminator Cycle Sequencing* kit using an ABI 377 DNA sequencer (Perkin-Elmer), all according to the instructions of the manufacturers.

Phylogenetic Analyses.—The SSU and ITS ribosomal DNA sequences are known to accumulate mutations (nucleotide substitutions) at very different rates and were used for different purposes. The SSU rDNA is typically subjected to a few substitutions fixed per million years. It allowed us to reconstruct a molecular phylogeny of the globorotaliid family. The *G. truncatulinoides* sequences were aligned to homologous genes of other globorotaliid species we cloned and sequenced for this study. This alignment was used to estimate the interspecific genetic variability between several morphological sister species whose fossil record is well known. The ITS genes, which evolve more rapidly, were then utilized to further analyze the intraspecific variability within *G. truncatulinoides.* Both SSU and ITS rDNA sequences were manually aligned, using the GDE 2.2 software (Larsen et al. 1993). Phylogenetic trees were reconstructed, based on 624 and 1121 unambiguously aligned sites for the ITS and SSU rDNA fragments, respectively, using both the maximum likelihood method with a transitions/transversions ratio of 2 (Olsen et al. 1994) and the neighbor-joining method (Saitou and Nei 1987) with genetic distances corrected for multiple hits from the Tajima and Nei model (Tajima and Nei 1984), as implemented in PHYLO_WIN (Galtier and Gouy 1996). This latter computer software was also used for computations of genetic distance. The NJPLOT program (Perrière and Gouy 1996) was used to plot phylogenetic trees. All new sequences reported in this paper have been deposited in the EMBL/GenBank databases (accession numbers AJ272474 to AJ272477 and AJ400152 to AJ400215) and their alignments are available on request to C. de V.

Restriction Fragment Length Polymorphism (RFLP) Analysis.—After DNA sequence analyses, a restriction enzyme that cuts the nucleotide sequence at a specific pattern was selected to rapidly discriminate between the different *G. truncatulinoides* genotypes. PCR-product digestions were performed using the endonuclease *Sau 96 I* (Roche), which cuts at the palindromic sequence G/GNCC, according to the following protocol: 12.5 μl of the PCR products from the total ITS region or the ITS-2 gene alone were directly digested for five hours at 37°C in a total volume of 25 μl containing 2.5 μl of the diluted enzyme (1.25 units), 2.5 μl of Buffer A (Roche), and 7.5 μl of distilled water. Distinct patterns for each genotype were UV detected after migration of the digested PCR products on a 2% agarose gel and ethidium bromide coloration.

Fourier Analysis of the Outline.—Fourier analysis has been used efficiently to describe the morphological variability of *G. truncatulinoides* (Healy-Williams and Williams 1981; Healy-Williams 1983; Healy-Williams et al. 1985). Shape analysis in our study was based on two-dimensional outlines, with two views providing a good approximation for the three-dimensional morphology: an edge view with the apertural face ahead and a spiral view. Outline extraction and Fourier analysis were performed with the OPTIMAS v. 5.0 image-processing software.

For each outline 64 points at equally spaced intervals were sampled. Starting points were defined at the edge of the last chamber for the edge view outline (lower right in Fig. 1), and the meeting point of the last chamber with the inner whorl for the spiral view outline. From these coordinates, 64 radii corresponding to the distance of each of the points to the center of gravity of the outline were calculated. A discrete Fourier analysis was then applied to this set of 64 radii, expressed as a function of the cumulative distance along the outline (Renaud and Girard 1999; Renaud et al. 1999a,b). The outline is thus expressed as a finite sum

of trigonometric functions of decreasing wave length, i.e., the harmonics, according to the formula

$$r(s) = a_0 + \sum_{n=1}^{K} [a_n \cos(s/L 2\pi n) + b_n \sin(s/L 2\pi n)] \quad (1)$$

where r is the radius at the abscissa s along the outline, L the perimeter, K the number of points along the outline, and n the rank of the harmonic. Each outline can, therefore, be described by a set of Fourier coefficients a_n and b_n, including both the amplitude ($= \sqrt{a_n^2 + b_n^2}$) and the phase ($= \arctan [b_n/a_n]$) information, and therefore representing a complete description of the outline. Size was standardized by dividing all coefficients by the 0th harmonic amplitude, a_0, which is proportional to the diameter of the best-fit circle to the digitized outline (Ehrlich and Weinberg 1970). A reconstruction of the outline corresponding to any set of Fourier coefficients was obtained using the Inverse Fourier Transform (Rohlf and Archie 1984).

The higher the order of the harmonic, the more detail of the outline it describes. This property can be used to filter measurement noise, expected to increase with the harmonic order (Renaud et al. 1996, 1999b). Measurement error was estimated by five repeated measurements on the edge and spiral views of a specimen, and expressed as the mean coefficient of variation of the harmonic amplitude. Results indicated a first increase in measurement error at the 6th harmonic and a second increase at the 12th harmonic for both views (Fig. 3). Higher harmonics include measurement error greater than 50% of the signal. The content of information added by each harmonic was also estimated using the cumulative power (Crampton 1995) as a function of the harmonic order. For both views, 95% of the total power is reached at the 12th harmonic. Therefore, we consider Fourier coefficients up to the 12th harmonic as a good compromise between information content and the limitations set by the measurement error. A set of 24 Fourier coefficients was consequently available from each outline for multivariate analyses. Edge and spiral views were treated separately, since both sets of coefficients correspond to different morphologic features in the tests of *G. truncatulinoides*, and because combining both would have led to a high number of variables incompatible with the limited sample size for several geographic groups (Table 1).

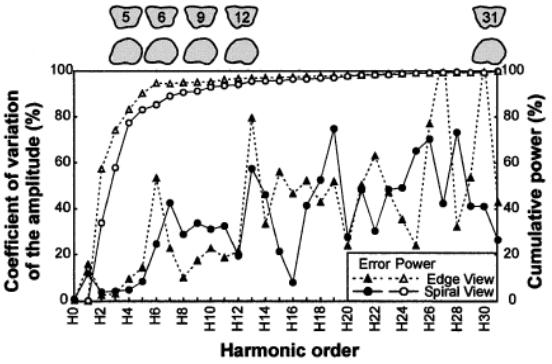

FIGURE 3. Measurement error and cumulative power as a function of the harmonic order. The measurement error (black symbols) is expressed as the coefficient of variation of the harmonic amplitude ($\sqrt{a_n^2 + b_n^2}$) for repeated measurements of the same specimen. Cumulative power (gray symbols) is the deviation of reconstructed outlines based on increasing numbers of harmonics from the reconstruction based on the maximum number of harmonics (H = 31), for both edge and spiral views. A few reconstructed outlines of edge and spiral views show the increasing details on the outlines corresponding to the increasing amount of information added by each harmonic.

We used a multivariate analysis of variance (MANOVA), associated with a canonical variate analysis, to display the morphological variability related to geographical patterns on a few synthetic axes. A test of significance for differences among groups relative to within-group variation (Wilk's Lambda test) and the scores of the individuals on the canonical axes are provided. The few individuals for which both morphology and genetics were available have then been projected as supplementary individuals on these canonical plots.

Size Analysis.—For comparison of size and shape variation, the amplitude of the 0th harmonic of the outline in spiral view, a_{S0}, was selected to represent the size of each specimen. Size in spiral view seems less sensitive to shape changes than the size in edge view. The relationship between a_{S0} and the diameter (D_S) derived from the perimeter in spiral view P_S, with $D_S = P_S/\pi$, was estimated. We found a

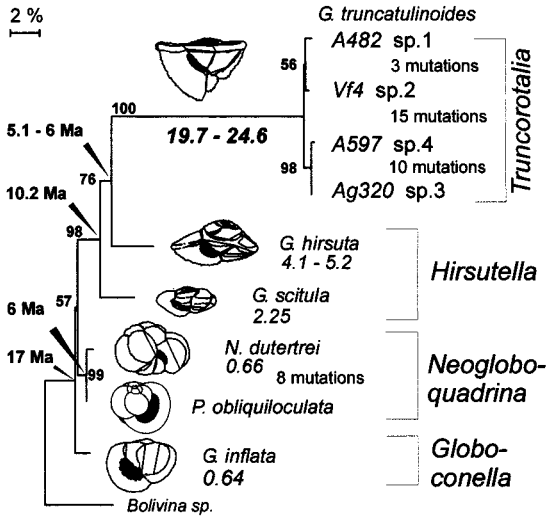

FIGURE 4. SSU rDNA-based evolutionary relationships between the four *Globorotalia truncatulinoides* genotypes, and representatives of several other globorotaliid species. This neighbor-joining tree is based on a *Tajima and Nei* genetic distances matrix computed from 624 unambiguously aligned sites. Tree topology is similar if the maximum likelihood method is used; bootstrap values greater than 50% are given next to the internal branches and the scale is in % of nucleotide differences. Divergence times given at some nodes of the tree are based on fossil data from the phylogenetic atlas of Kennett and Srinivasan (1983). Molecular rates of evolution (in italics) are given in substitutions/1000 bp/m.y. Subgenus names according to Kennett and Srinivasan (1983).

significant linear correlation between both variables: $r^2 = 0.982$, $p < 0.001$; $a_{S0} = 0.135 + 3.186\ D_S$.

Molecular Position and Age of the *G. truncatulinoides* Genotypes within the Globorotaliids

A Globorotaliid SSU rDNA-Based Phylogeny.— We started by sequencing the SSU rDNA from several *G. truncatulinoides* specimens along the AMT transect, and from five other globorotaliid morphospecies: *Globorotalia inflata*, *G. scitula*, *G. hirsuta*, *Neogloboquadrina dutertrei*, and *Pulleniatina obliquiloculata* (Fig. 4). The SSU rDNA is a conservative gene that has been used for studies of the phylogeny of morphologically defined species of foraminifera (de Vargas et al. 1997; Pawlowski et al. 1997; Darling et al. 1999). The relatively low rate of substitution in the SSU rDNA allowed us to align and compare the different globorotaliid homologous sequences, except in a few parts of the six variable areas of the gene (Fig. 2).

The molecular phylogenetic relationships obtained between the different globorotaliid species (Fig. 4) reflect the current phylogenetic interpretations of their fossil record based on morphological and stratigraphic analyses, although clear interlineage differences in rates of DNA substitution occur, as revealed by the high disparities in the branch lengths of the tree.

The evolutionary sequence *Globorotalia scitula–G. hirsuta–G. truncatulinoides*, supported by 98% and 76% bootstrap values (Fig. 4), is congruent with the stratophenetic hypotheses of Stanley et al. (1988, based on Kennett and Srinivasan 1983) and Bolli et al. (1985); it also fits the cladistic analysis of Norris et al. (1994). The divergence time of the subgenus *Truncorotalia* from *Hirsutella* can be estimated from the stratigraphic record, but it depends on whether *G. cibaoensis* and *G. juanai* (Kennett and Srinivasan 1983) or *G. crassula* and *G. margaritae* (Bolli et al. 1985) are considered as first members of the *G. truncatulinoides* and *G. hirsuta* lineages, respectively. The *Globoconella* clade, leading to *G. inflata*, is widely accepted as having emerged ~17 Ma from *G. praescitula*, the direct ancestor of *G. scitula* (Kennett and Srinivasan 1983). The close relationship between the *N. dutertrei* and *P. obliquiloculata* lineages (sustained by a 99% bootstrap value in the molecular tree) and their separation from *N. acostaensis* ~6 Ma are also well documented from sediments (Kennett and Srinivasan 1983; Bolli et al. 1985).

The relative positions of the three statistically well-supported groups, *Hirsutella-Truncorotalia, Globoconella*, and *Neogloboquadrina*, are not resolved in our analysis (bootstrap value of 57%). The unequal rates of DNA substitution along the different lineages probably obscure the topology at this basic level of the tree. If the fastest-evolving species, *G. truncatulinoides*, displaying the longest branch, is removed from the analysis, we obtain an ancestral position of the *Neogloboquadrina* clade with the maximum likelihood method (the less sensitive method to the artificial ''long branch attraction'' phenomenon). This is congruent with the hypothesis that the *Neoglobo-*

quadrina genus emerged from *N. continuosa* (Kennett 1983 and Srinivasan), whose first appearance dates from the early Miocene.

Four Different Genotypes of G. truncatulinoides.—We obtained four different SSU rDNA sequences from *G. truncatulinoides*, separated by small but significant genetic divergences (13–54 nucleotide substitutions), and tentatively designated as spp. 1, 2, 3, and 4. The *G. truncatulinoides* clade is thus characterized by a very long branch leading to a main dichotomy that generates two groups: (sp. 1–sp. 2) and (sp. 3–sp. 4). This branching pattern is identical in all analyses.

Calibration of the Globorotaliid Molecular Tree Using the Fossil Record.—Since the globorotaliid molecular phylogeny is highly congruent with the fossil data, it was possible to calibrate most nodes of the molecular tree with ages from the fossil record (Fig. 4). This allows calculation of rates of DNA substitution along the internal and terminal branches of the tree, by dividing the length of the branches (number of mutations) by the stratigraphic time period attributed to each branch. *Globorotalia truncatulinoides* is already known to be a ''fast-clock'' species (de Vargas and Pawlowski 1998) that fixes mutations at an even higher rate than the spinose planktic foraminifera, which otherwise have the highest substitution rate recorded to date for the SSU rDNA (Pawlowski et al. 1997). The current analysis confirms the very high DNA substitution rate in the *G. truncatulinoides* lineage, 30 to 40 times higher than the rates calculated for the *Neogloboquadrina* or *Globoconella* clades (Fig. 4). Moreover, our analysis shows that the acceleration of substitution rate is not an aberrant feature of *G. truncatulinoides* alone. It already exists in the older *Hirsutella* lineages, which are indirect ancestors of *G. truncatulinoides.* The *G. scitula* lineage evolved about three times faster than *N. dutertrei* or *G. inflata* lineages, and about two times slower than the *G. hirsuta* lineage. Thus it seems that rates of mutations increase in the phylogenetic direction of *G. truncatulinoides.*

To estimate the separation times of the different *G. truncatulinoides* genotypes, we used the specific substitution rate calculated for its lineage of 19.7–24.6 subst./1000 bp/m.y., and assumed that DNA mutations accumulated with a clocklike behavior since the origin of the species. The split between (sp. 1–sp. 2) and (sp. 3–sp. 4) would have occurred between 263 and 329 Ka.

TABLE 2. Pairwise genetic distances-in % of nucleotide differences-separating the four genotypes of *G. truncatulinoides* for each ribosomal region analysed in this study. The 5.8S gene is the most conservative, followed by the SSU, and then the ITSs; this ranking is inversely proportional to the G + C content of those genomic areas (Fig. 2). A linear regression analysis of the respective genotypic pairwise distances between the different genes indicates that the ITS sequences evolve, as a mean value, ~5 times faster than the SSU rDNA, while the 5.8S sequences change 1.7 times slower than the SSU rDNA.

Pairwise comparison	Observed and Tajima and Nei (1984) genetic distances			
	SSU rDNA	ITS-1 rDNA	ITS-2 rDNA	5.8S rDNA
sp.1/sp.2*	3.5/3.6	13.8/15.4	14.0/15.8	2.1/2.2
sp.1/sp.3	6.2/6.5	24.8/31.0	24.4/29.9	2.7/2.7
sp.1/sp.4	5.8/6.0	25.5/32.0	24.4/30.6	2.7/2.7
sp.2/sp.3	6.2/6.5	25.5/31.7	25.6/32.1	4.8/5.0
sp.2/sp.4	6.0/6.3	25.0/30.8	26.0/32.8	4.8/5.0
sp.3/sp.4*	1.2/1.2	10.3/11.2	8.1/8.7	1.1/1.1

* The *G. truncatulinoides* A482, Vf4, Ag320, and A597 (Fig. 4) were used for distance computation.

Genetic Variability within *G. truncatulinoides*

ITS Genes, a Tool for Studying Recent Speciation Events.—Too few DNA substitutions separate the *G. truncatulinoides* genotypes in the SSU rDNA for an accurate estimation of their genetic differentiation. Therefore, for the first time in planktic foraminifera, we used the ITS ribosomal DNA (ITS rDNA; Fig. 2), which is known to evolve much faster than the SSU rDNA, to further determine the genetic variability within the *G. truncatulinoides* cluster.

Again, four distinct genotypes were observed (Fig. 2). Their main structural differences are in the ITS-2 gene, with several genotype-specific DNA fragment insertions and deletions, including a 104 bp duplication in sp. 2. The inter-genotype genetic distances are much higher for the ITS rDNA than for the SSU rDNA (Table 2). For the whole ITS region, the observed genetic distances between genotypes are significant: 11.3% between sp. 1 and sp. 2, 8.3% between sp. 3 and sp. 4, while (sp. 1–sp. 2) is 19.5% divergent from (sp. 3–sp.

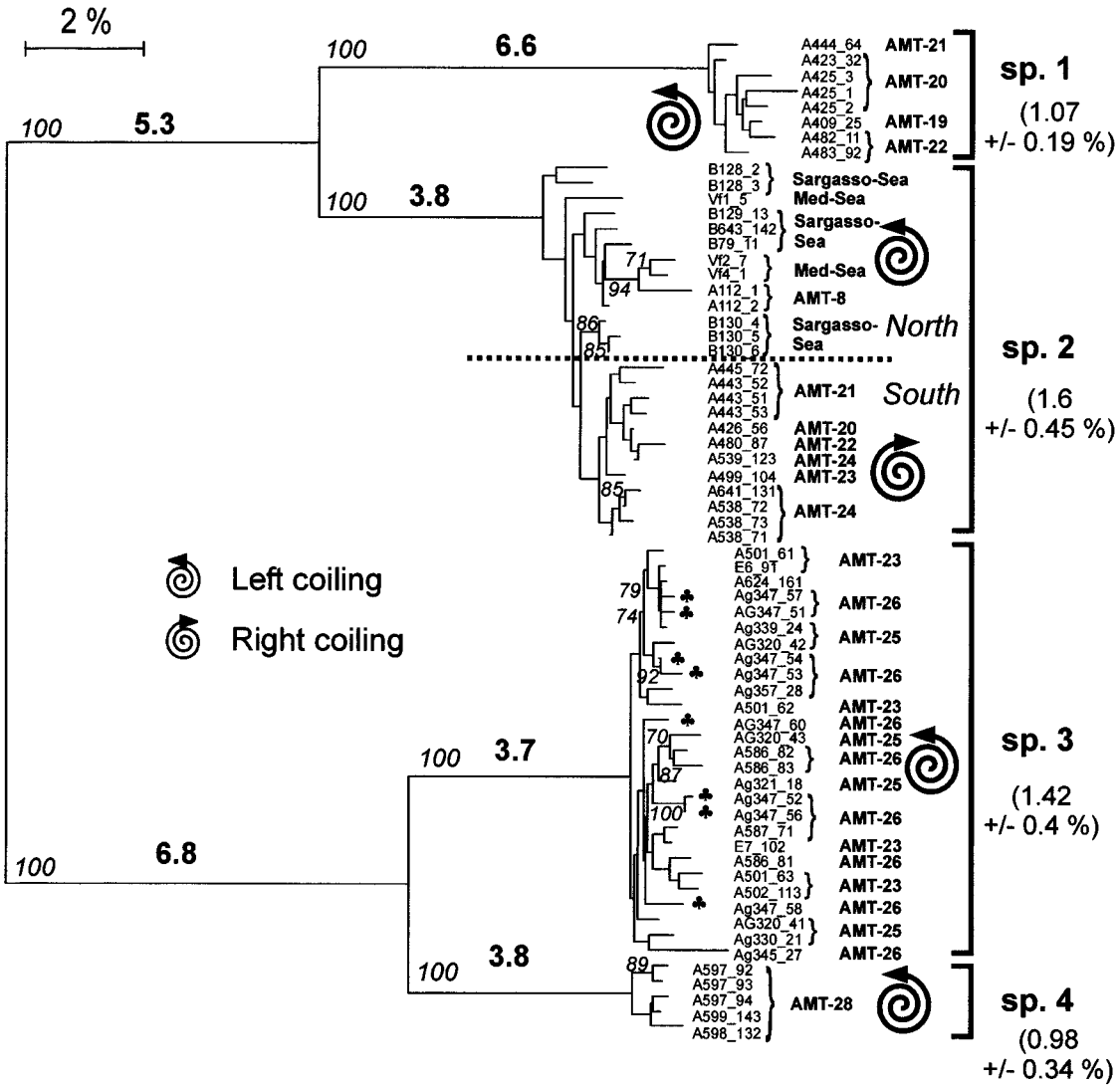

FIGURE 5. ITS-based evolutionary relationships between 65 clones of *Globorotalia truncatulinoides* from 12 localities in the Atlantic Ocean and Mediterranean Sea (see Table 1 and Fig. 9 for station names and locations). This neighbor-joining tree is based on *Tajima and Nei* genetic distances using 1121 unambiguously aligned sites. Bootstrap values greater than 70% are given in italics next to each internal branch, and the scale and branch lengths (in bold) are in % of nucleotide differences. Within-genotype mean genetic variabilities with standard deviation are given in brackets on the right of the four clades. In the sp. 3 cluster, a black clover indicates eight clones sequenced from the same individual at AMT-26. Divergence times are inferred from the molecular clock.

4). This last distance represents ~170 DNA substitutions.

ITS-Based Phylogenetic Analysis.—Sixty-five ITS rDNA's from 40 individuals from various localities have been cloned, sequenced, and phylogenetically analyzed for estimating *G. truncatulinoides* inter- and intra-individual genetic variability (Fig. 5). The clones cluster in four largely divergent groups (the species 1, 2, 3, and 4) supported by 100% bootstrap values. A mean genetic variability of 1–1.5% separates the clones within each group. This intragroup variability, low in comparison to the genetic distances between the main genotypes, does not disturb the principal, more basic phylogenetic relationships. The branching pattern (sp. 1–sp. 2)/(sp. 3–sp. 4) is identical in all analyses and confirms the topology resulting

from the SSU rDNA analyses (Fig. 4), despite the highly different structural evolutionary constraints on both DNA regions.

Genetic Variation at the Allelic Level.—An important feature of the *G. truncatulinoides* ITS genes is the variability between the multiple copies amplified from an individual genome (note for instance the eight distinct clones of the cell *Ag347* in Fig. 5), as described for the LSU rDNA in the benthic foraminifer *Ammonia* (Holzmann et al. 1996). We never found any identical sequences in our 65 clones. This intra-individual variability suggests independent evolution of the multiple copies within a genome since the origin of the common ancestor of the analyzed cells. Moreover, the substitution rate of the ITS region is high enough to override the phenomenon of ''concerted evolution,'' which tends to equalize—likely by mechanisms of unequal recombination—the paralogous rDNA sequences.

Ecological Preferences of the Four *G. truncatulinoides* Genotypes

Hydrography along the Transect.—The southwestern Atlantic region we sampled is characterized by the confluence of the warm, saline, and oligotrophic southward Brazil Current (BC) and the cool, dense, and nutrient-rich northward Falkland Current (FC). The AMT transect also crossed oceanic areas that can be strongly influenced by the estuarine, fresh, and warm waters from the Rio de la Plata (RP) (Willson and Rees in press). The first derivative of near-surface water density has been used as an indicator of water masses on several AMT cruises (Hooker et al. in press) and indicates five different provinces between stations AMT-19 and AMT-28 (Table 1). The BC/FC confluence zone (34–44°S) is extremely heterogeneous with the continuous formation, in both south and north directions, of eddies and filaments containing FC, BC, or RP waters in different proportions. Willson and Rees (in press) integrated satellite-derived sea-surface height anomaly (TOPEX) and sea-surface temperature (AVHRR) data with AMT-5 in situ measurements to identify positions and properties of the eddies present during our sampling period. Between 34°S and 44°S, the ship track went across an assortment of eight different eddies (Fig. 6) derived from waters of subtropical to polar origin. The scale of our sampling (~280 km spacing) was unfortunately relatively coarse when compared with the eddy scale of typically 50 km in diameter. However, the oceanographic logger (Fig. 6), and the CTD data from each station (Fig. 7), allowed us to identify the water-mass features at each collected locality out of this complex network.

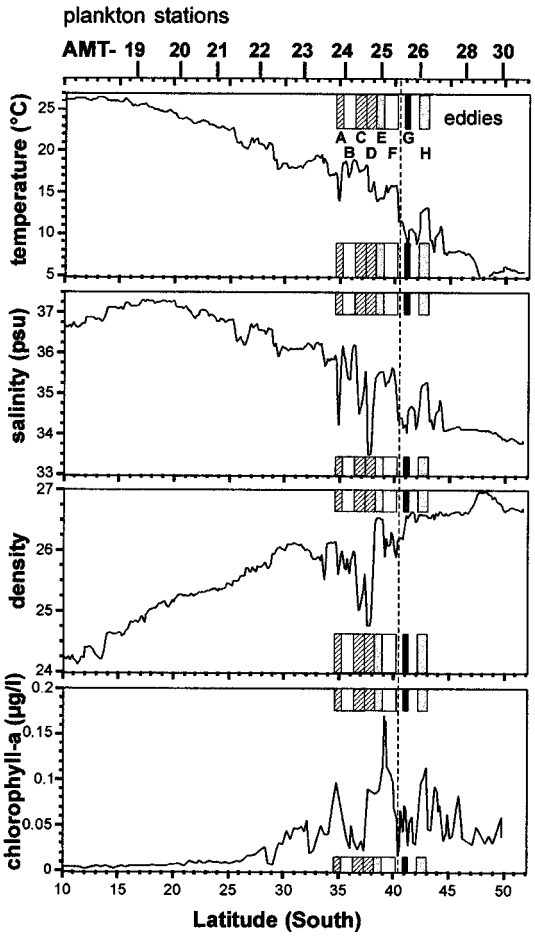

FIGURE 6. Sea-surface hydrographic parameters for the Southern Hemisphere part of the AMT-5 transect (logger data). Locations of the plankton sampling sites are indicated on top of the graphs. In the mixing zone between the Brazil Current (BC) and the Falkland Current (FC) (34°–44°S), eight eddies of different hydrographic characteristics (A to H) (Wilson and Rees in press) are latitudinally located with rectangles: white = BC subtropical waters (B, F); hatched = River Plate influence (A, C, E); black = FC subpolar waters (G); gray = FC/BC mixed waters (B, F). AMT-24, 25, and 26 fall in eddies B, E, and H. The Subpolar Front is indicated by a hatched line located at ~40°S.

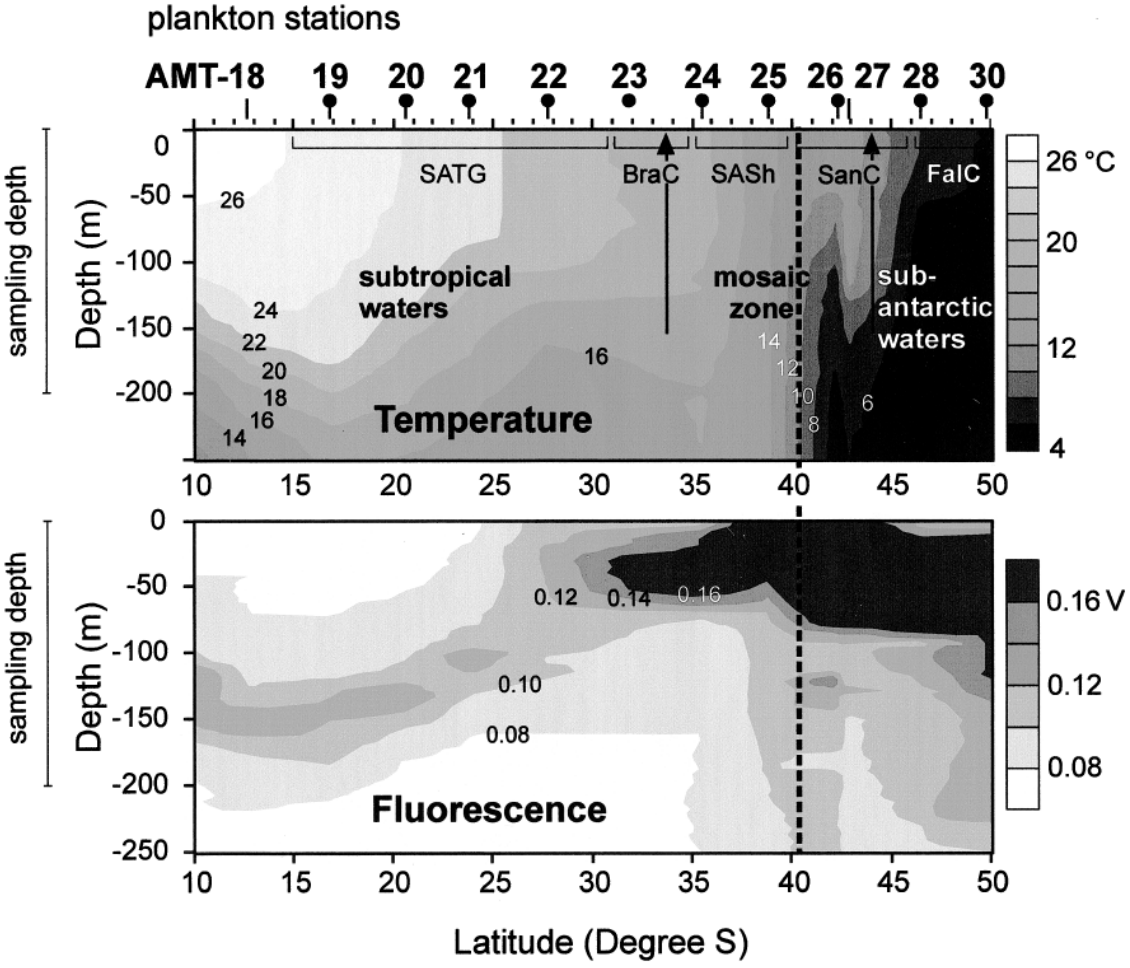

FIGURE 7. Temperature and fluorescence (used here as a proxy of chlorophyll concentration) variations to a depth of 250 m along the Southern Hemisphere part of the AMT-5 transect. Locations of the sampling sites are indicated on top of the graphs, as well as the oceanic provinces as defined by Hooker et al. (in press) (Table 1). The Subpolar Front is indicated by a hatched line located at ~40°S.

Distribution of G. truncatulinoides Genotypes.– The distribution of all specimens of *G. truncatulinoides* characterized either by sequencing or RFLP (Fig. 8) is illustrated in Figure 9. While only sp. 2 occurred in the North Atlantic at different times of the year, all four genotypes were present in the South Atlantic during the same season. Half of the AMT stations contained two or more genotypes in sympatry. Our genotype mapping is only a snapshot of the seasonal and spatial variation and our sampling does not discriminate between depth intervals in the water column. However, the relationships between the four genotypes and oceanographic features suggest that their distribution is controlled by environmental parameters.

Sp. 1 and sp. 2 co-occur in the stations AMT-19 to AMT-22, in subtropical waters dominated by the Brazil Current. Temperature and salinity in the mixed layer are relatively high (>20°C and >35‰; Figs. 6, 7) with a gradual decrease southward. A weak deep chlorophyll maximum rises from ~150 m to ~100 m depth between AMT-19 and AMT-22 and is clearly associated with the top of the seasonal thermocline (Fig. 7).

Sp. 1, sp. 2, and sp. 3 are mixed at AMT-23. Unfortunately, CTD data are not available for this station. However, the relatively high chlo-

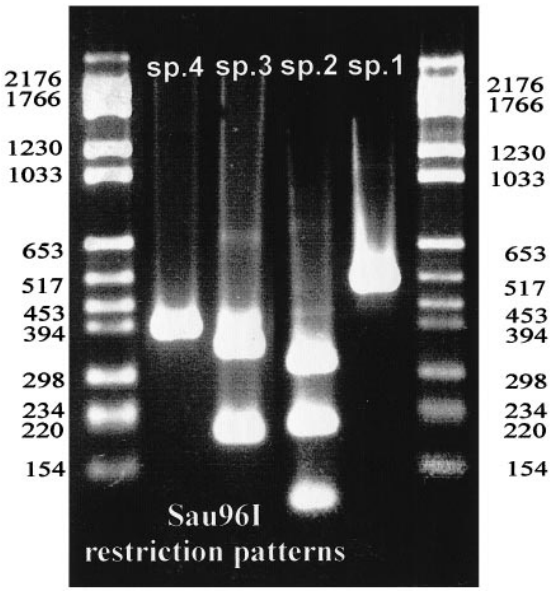

FIGURE 8. Restriction patterns resulting from RFLP analyses on ITS-2 PCR products, using the endonuclease Sau96 (Roche). Each *Globorotalia truncatulinoides* genotype has its specific pattern and can be detected at first glance.

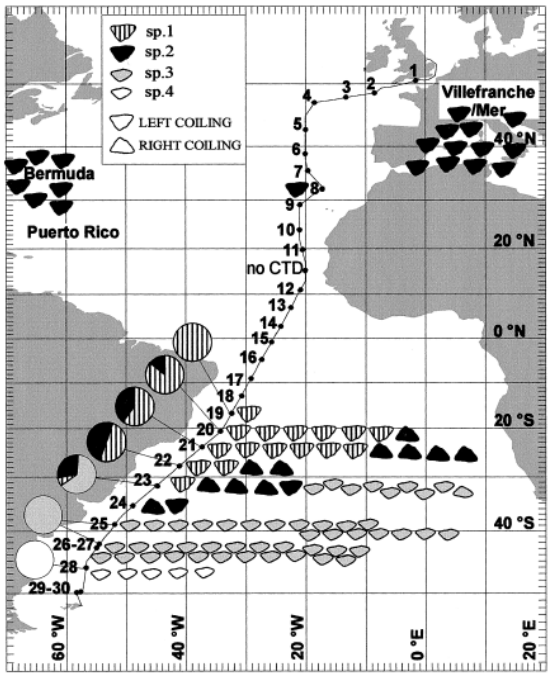

FIGURE 9. Geographic distribution of the four *Globorotalia truncatulinoides* genotypes. Each symbol depicts a single genetically characterized individual. The ratio of the different genotypes between stations AMT-19 and AMT-28 is also expressed in pie charts.

rophyll concentration in the surface waters at this site (Fig. 6) suggests a mixing of subpolar and subtropical water masses in this area that may explain the presence of the three genotypes.

At AMT-25 and AMT-26 only sp. 3 was present in abundance. These sites are located on both sides of the Subantarctic Front (which is indistinguishable from the Subtropical Convergence in this part of the ocean), as shown by the 9°C drop of temperature between 40°S and 41°S and the vertical water structure in this area (Fig. 7). Both stations are located in eddies of similar hydrographic properties (eddies E and H of William and Rees [in press]), whose salinity and temperature are intermediate between typical BC and FC values, leading to water density close to that of the subpolar water mass (Fig. 6). AMT-25 and 26 are representative of the Subantarctic Convergence province, characterized by extreme heterogeneity and very rapid changes in water properties in latitudinal and vertical directions. The intense vertical mixing in this unstable surface water mass supports high productivity in near-surface waters through input of nutrients from depth (Fig. 7).

Sp. 4 was restricted to AMT-28. This station is typical of the Falkland Current province, where cold and nutrient-rich subantarctic surface water flows northward. The temperature and salinity are low (8°C and 34‰) and stable until 250 m depth; the vertical chlorophyll concentration profile resembles the pattern in stations AMT-25 and 26 (Fig. 7).

Morphological Variability

Genetic analyses of unicellular organisms are usually disruptive and do not allow combined DNA and morphometric analyses. In this study, the relationships between morphometric characteristics and genotypes are, therefore, largely based on compared patterns of geographic distribution, except for six individuals on which we tested a new nondisruptive method of DNA extraction.

Size Differentiation.—The size of *G. truncatulinoides* varies with geographic position (ANOVA on a_{S0}: $F = 10.646$; df = 9; $p < 0.001$). Although small samples from the northern stations limited the interpretation, larger max-

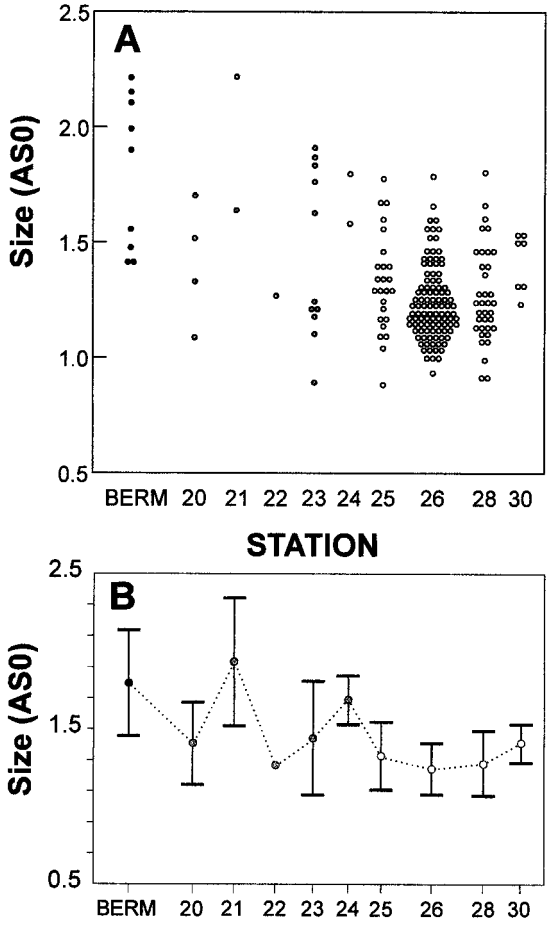

FIGURE 10. Geographic variation in size, estimated by the 0th harmonic amplitude of the spiral view. A, Distribution of the size measurements for each station. B, Variation of the mean size ± standard deviation.

imum test size seems to occur in the subtropical stations (Bermuda, AMT-20 to AMT-23). The size distribution at the Subantarctic Convergence and subpolar water stations (AMT-25, 26, 28) is skewed toward smaller sizes, corresponding to smaller mean size (Fig. 10).

Shape Differentiation.—MANOVAs on the Fourier coefficients indicate a morphological differentiation between specimens from different stations, for both edge and spiral views (edge view: *Wilk's* $\lambda = 0.075$; *Approx-F* = 2.426; df = 216, 1466; $p < 0.0001$; spiral view: *Wilk's* $\lambda = 0.175$; *Approx-F* = 1.525; df = 216, 1440; $p < 0.0001$).

In edge view (Fig. 11A), the position of the different group means along the first canonical axis (54% of the among-group variance) discriminates between subtropical assemblages (Bermuda, AMT-21 and AMT-24) and those from stations across the Subantarctic Convergence and subpolar water masses (AMT-25, 26 and AMT-28, 30, respectively). AMT-20 and AMT-23 are in an intermediate position. The second canonical axis mostly separates AMT-20 and AMT-30. The reconstructed outlines illustrate the shape changes involved in the morphological differentiation: highly conical tests with flat or concave spiral sides are characteristic of subtropical stations, while less conical tests with a raised spiral side occur in cold-water stations.

Outlines in spiral view (Fig. 11B) lead to the same discrimination between subtropical sites, including AMT-20, and the frontal and subpolar stations along the first canonical axis. AMT-23 holds an intermediate position again. The reconstructed outlines show more angular shapes with a large protruding last chamber for subtropical stations and more compact, round outlines for frontal and subpolar stations.

To further evaluate the morphological variability at each station, all individuals have also been represented per station in the canonical space for both edge view (Fig. 11C) and spiral view (Fig. 11D). The populations appear to be homogeneous at each site. The clear morphologic differentiation between individuals of northern subtropical and southern stations is mainly expressed in edge view. For both views, specimens from AMT-23 display a high variability, ranging across the segregation zone.

Size and Shape Relationship.—To consider the possible influence of size on shape differentiation we compared scores on the first canonical axis of edge and spiral view with the size parameter a_{S0}. A strong relationship seems to exists between shape and size in the morphological space defined by these variables (Fig. 12A,B). Subtropical specimens with highly conical and angular tests from Bermuda, AMT-21, and AMT-24 are also characterized by large size. However, for similar size, specimens from the subtropical station AMT-20 (and AMT-23 for some individuals) are still morphologically different from specimens

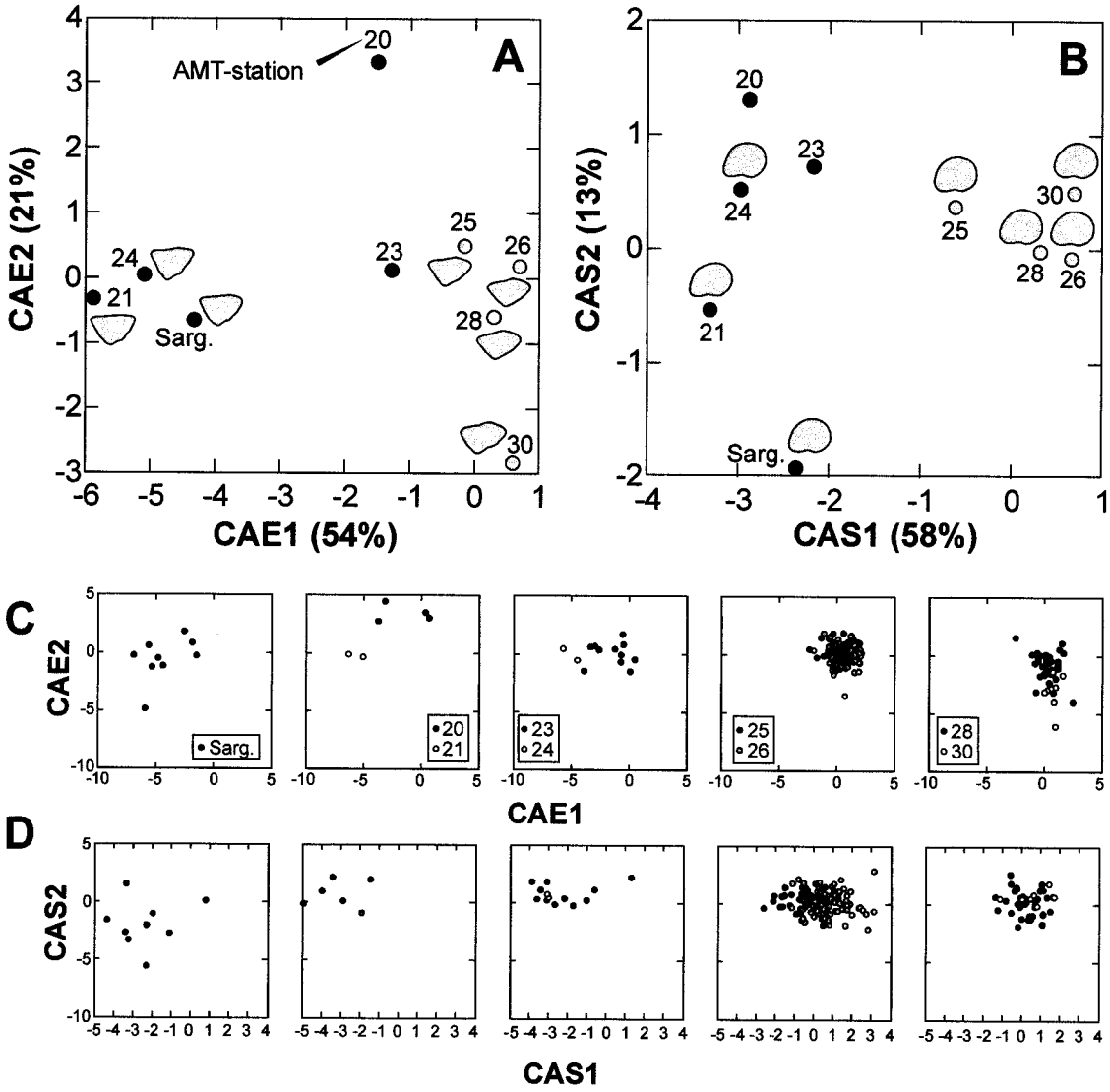

FIGURE 11. Shape variations. A, Relationships between group (all individuals from one station) means on first two canonical axes corresponding to the edge view of *G. truncatulinoides* (CAE1 and CAE2). Reconstructed outlines for some group means visualize shape changes. B, Relationships between group means of the spiral view (CAS1 and CAS2). C, Morphological variability within each station for the edge view. D, Idem, spiral view.

collected across the Subantarctic Convergence and subpolar stations AMT-25 to 30, mainly in spiral view.

The size-shape relationships for all individuals are shown in Figure 12C and 12D. While the frontal zone and subpolar populations do not show any obvious allometric relationship, the subtropical specimens are more conical and angular with increasing size.

Linking Morphometric and Genetic Analyses.—Similar patterns of morphological and genetic differentiation can be recognized. The geographic distribution of the genetic group (sp. 1–sp. 2) matches the distribution of the subtropical morphological group, while the genetic group (sp. 3–sp. 4) corresponds to the frontal and subpolar morphology. Corroborating this association, station AMT-23 yielded a mixed assemblage of three genotypes that may explain its morphologically intermediate position as a result of mixing.

An experimental, nondestructive procedure

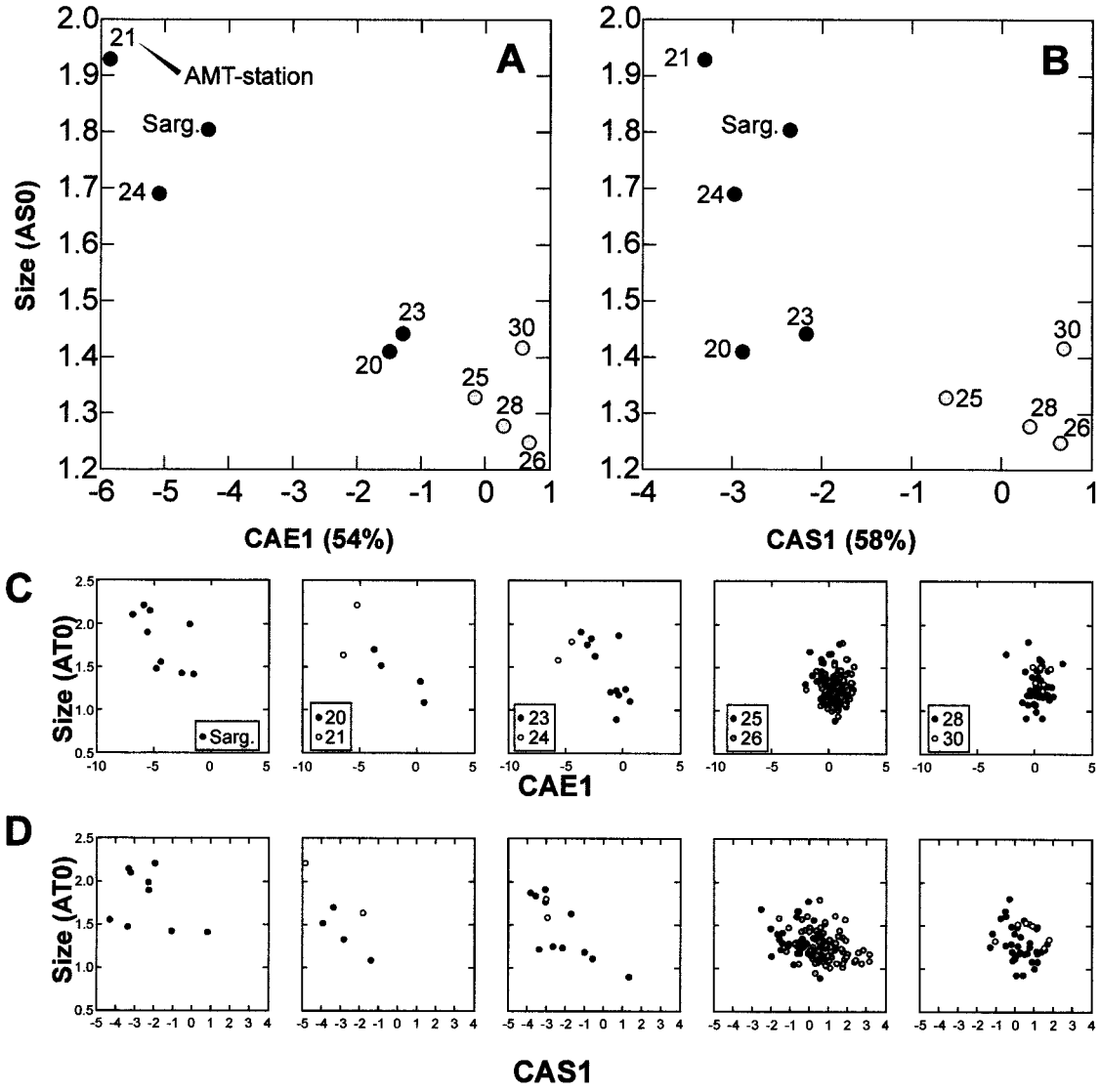

FIGURE 12. Relationship between size and shape, represented by first canonical axes for edge and spiral view. A, Among-group size-shape relationship, edge view. B, Idem, spiral view. C, Within-group allometry, edge view. D, Idem, spiral view.

of DNA extraction allowed us to confirm this hypothesis of a link between the main genetic and morphological differentiation. The outlines of six specimens (Fig. 13A), genetically attributed to sp. 1, sp. 2, and sp. 3, have been analyzed and plotted in the canonical spaces previously defined by the morphometric analyses. The pattern is especially clear in edge view (Fig. 13B), where specimens of sp. 1 and sp. 2, from AMT-21 and 23, morphologically fall within the range of variation observed at subtropical stations. Sp. 3 specimens, collected from the frontal environment, are morphologically close to the assemblage from the frontal and subantarctic, cold-water stations. The morphological discrimination is less clear in spiral view (Fig. 13C), where a larger overlap between warm-water and cold-water populations exists, but confirms the existence of a link between subtropical and frontal/subpolar populations, and the main genetic dichotomy separating (sp. 1–sp. 2) from (sp. 3–sp. 4) (Fig. 5).

Coiling Direction.—No significant difference

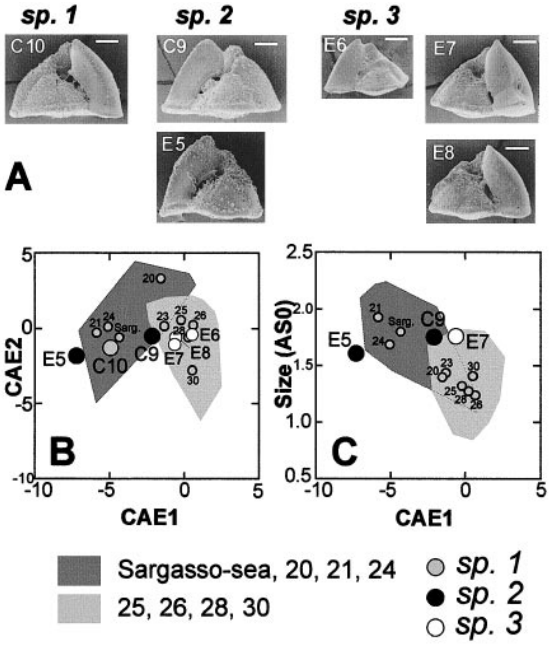

FIGURE 13. Relationship between genetics and morphology. A, SEM edge view of the six *G. truncatulinoides* specimens from which DNA was extracted without shell destruction. Scale bars, 100 μm. B, Location of the six specimens (A) in the canonical space, based on morphometric analysis of the edge view. Means of the different stations are reported, as well as the morphological range of variation of subtropical stations (dark gray) and frontal to subpolar stations (light gray). C, Idem, spiral view.

in outline shape discriminates between *G. truncatulinoides* sp. 1 and sp. 2 in our analysis. However, sp. 1 and sp. 2 differ in the coiling direction of their tests between 16°S and 31°S (~1200 km). The tests of all sp. 1 individuals genetically determined in this geographic range are left-coiled ($n = 16$), while all tests of sp. 2 ($n = 12$) are right-coiled, except for one. Between AMT-19 and AMT-22 the total abundance of left-coiled (sp. 1) individuals in *G. truncatulinoides* was 1 of 1, 15 of 16, 7 of 12, and 4 of 8 (or 100%, 93%, 58%, and 50%). This may indicate some decrease in abundance of sp. 1 from north to south during the time of the cruise.

Discussion

Globorotalia truncatulinoides as a Complex of Four Genetic Species.—The analysis of both the highly conservative SSU rDNA and the rapidly evolving ITS rDNA reveals the existence of four different genotypes within *G. truncatulinoides* in the Atlantic Ocean (Figs. 4, 5). Several pieces of evidence indicate that these genotypes may correspond to fully isolated species between which gene flow was interrupted during the past few hundred thousand years: (1) The different ITS rDNA alleles found within individuals do scatter among sequences from other individuals of the same genotype, but they never branch with sequences from another genotype despite sympatric occurrence of different genotypes at several stations. (2) The intra-genotype genetic distances, although tested at a large geographic scale (particularly for sp. 2), are very low compared to the inter-genotype distances. (3) The genetic distances between genotypes are large relative to the mutation rates (~8 and 40 DNA substitutions every 100,000 yr in a 1000-bp DNA fragment for the SSU and ITSs rDNA, respectively). (4) Those genetic distances are of the same order of magnitude as distances separating clearly distinct morphological species of planktic foraminifera (Fig. 4).

Moreover, the use of ITS rDNA sequences allowed us to identify structured genetic variability at the intra-genotype level. The clones of sp. 2 cluster in two groups: those from the Mediterranean, Bermuda, and AMT-8 (18°N), and those from the Southern Hemisphere stations AMT-20 to AMT-24 (20°S to 35°S) (Fig. 5). This intra-genotype genetic differentiation is even associated with a morphologic change from a northern left-coiled population to a southern right-coiled population, and likely reflects differentiation of geographic populations (or recent subspecies). This further supports the idea that the deepest nodes in the ITS rDNA-based tree correspond to at least the species level of differentiation.

The Molecular-Clock Timing Fits the Stratigraphic Record.—According to the SSU rDNA molecular clock (Fig. 4), the different genetic species are relatively young. The first genetic split between the subtropical group (sp. 1–sp. 2) and the Subantarctic Convergence and subpolar group (sp. 3-sp. 4) would have happened ~300 Ka. Too few mutations separate sp. 1 from sp. 2, and sp. 3 from sp. 4, in the SSU rDNA to accurately infer their divergence time. However, by assigning 300,000 yr to the deepest dichotomy in the ITS rDNA-based

phylogeny (Fig. 5), the molecular clock indicates ages of ~170 Ka and ~120 Ka for the sp. 1/sp. 2 and sp. 3/sp. 4 divergences. Our molecular timing of the earliest genetic splitting is congruent with stratigraphic studies, which indicate a first appearance of compressed forms of *G. truncatulinoides* in northern subantarctic waters at 300–200 Ka (Kennett 1970). Our data suggest that this acclimatization of the species to subpolar water masses, coincident with the appearance of a new compressed morphotype (the end-member morph of the modern latitudinal cline), corresponds in fact to an adaptive speciation.

Morphological and Environmental Differentiation within the G. truncatulinoides Species Complex.—The genetic differentiation between (sp. 1–sp. 2) and (sp. 3–sp. 4) is associated with a clear morphological differentiation (Figs. 11, 13). Subsequent speciation events, leading to two subtropical, a frontal, and a subpolar species, are probably too recent to be associated with any obvious morphometric differentiation of their outline (Fig. 11). However, sp. 1 and sp. 2 are at least clearly differentiated in their coiling directions between 16°S and 32°S (Fig. 9), and the absence of any identifiable outline discrimination might be due to their insufficient sampling. Moreover, outlines are a fraction of the total morphologic information available for examination and differences may exist in ultrastructural or ontogenetic characters of the test.

Our data suggest that the different species of the *G. truncatulinoides* complex have specific ecological preferences. The appearance of the ancestor of sp. 3 and sp. 4 is obviously linked to a biogeographic and environmental differentiation. At ~300 Ka, this new species, morphologically similar to our (sp. 3–sp. 4), invaded the northern subantarctic province, characterized by nutrient-rich, cold, weakly stratified and productive waters (Kennett 1970; Pharr and Williams 1987) (Fig. 7).

Within the cluster (sp. 3–sp. 4), sp. 3 lives in the subantarctic frontal system under conditions of strong vertical mixing, unstable water masses, high nutrient availability, and resultant productivity, while sp. 4 was collected in typical cold, dense, nutrient-rich, and productive subpolar waters (Figs. 7, 9).

Ecological preferences of sp. 1 and sp. 2 are more difficult to determine. Both genotypes were found in the same samples from the Brazil Current waters, where subtropical water is stratified and includes a distinct deep chlorophyll maximum (Fig. 7). Therefore a vertical niche differentiation of the two genotypes cannot be excluded as we did not perform depth-stratified plankton tows. Our sampling sites may also correspond to a geographic (or seasonal) mixing zone between the two species, whose biogeographic centers would be separated elsewhere (or at an other time) in the subtropical ocean. Thiede (1971) demonstrated that left-coiled subtropical *G. truncatulinoides* tests are larger and are found in greater abundance far from the land than the right-coiled tests. This may suggest that left-coiled sp. 1 inhabits more central nutrient-depleted regions of the subtropical ocean, while right-coiled sp. 2 is characteristic of environments with phytoplankton blooms (margins of subtropical gyres, coastal upwelling near France, island effect near Bermuda; see Fig. 9). This hypothesis is also congruent with the latitudinal relative abundance of right-coiled (sp. 2) *G. truncatulinoides* from South Atlantic surface sediments (Mulitza et al. 1997: Fig. 2B).

Reconsidering G. truncatulinoides Morphological Variations in Holocene Sediments.—Analyses of size distribution (Lohmann and Schweitzer 1990), isotopic composition (Mulitza et al. 1997; Hemleben et al. 1985), or abundance (Martinez 1997) of the shells from Recent sediments or plankton tows reveal differences within *G. truncatulinoides* (as a morphospecies) in depth habitat, seasonal occurrence, or biogeography. These observations have usually been attributed to ecophenotypic variations and to a complex life cycle—during which the species undergoes a very deep migration to release its offspring at ~600 m depth before death—within a single species. However, Healy-Williams and collaborators (Healy-Williams and Williams 1981; Healy-Williams 1983; Healy-Williams et al. 1985) applied morphometric analyses to more than 2400 *G. truncatulinoides* specimens from 20 surface-sediment samples collected between 22°S and 47°S in the Indian Ocean. They described three distinct groups characterized by specific outlines

in edge view and coiling ratio, and by distinct maximum abundance in the subtropical water mass, the Subtropical Convergence, and the subpolar water mass. Moreover, ratios of stable oxygen isotopes incorporated in their tests suggest the subtropical population resides (or, if the $\delta^{18}O$ signal of the analyzed shells was masked by gametogenic crusting, at least reproduces) at greater depth, likely in the deep chlorophyll maximum of relatively warm waters, while the more compressed tests of the populations in the Subtropical Convergence and subantarctic waters calcified in shallower, cold, and nutrient-rich waters. Stable carbon isotopes also indicate different vital effects in the three groups (Healy-Williams et al. 1985).

Our data from living *G. truncatulinoides* strongly support the results of Healy-Williams and collaborators. We differ in the recognition of four distinct species instead of three different populations in the considered zone. The morphopopulation of right- and left-coiled subtropical specimens from 16–28°S described by Healy-Williams et al. (1985) includes our sp. 1 and sp. 2, as suggested by their similar outlines and coiling characteristics, biogeographic occurrences, and environmental preferences (Healy-Williams et al. 1985 versus our Figs. 7, 8, 9, 11). Still, a significant difference in shape between left and right-coiled subtropical (29°S) specimens recognized by Healy-Williams et al. (1985) suggests the existence of a slight morphological differentiation between sp. 1 and sp. 2.

According to our morphologic, ecologic, and biogeographic analyses, sp. 3 and sp. 4 correspond to the frontal system and subpolar populations described by Healy-Williams et al. (1985). Isotopic analyses (Healy-Williams et al. 1985; Mulitza et al. 1997) suggest that both species inhabit surface waters where the nitrate/nitrogen levels are approximately five times those of subtropical waters, in contrast to low latitudes forms, which would live and/or reproduce deeper in the water column. This interpretation matches with the hydrographic distribution of the genetic species (Figs. 7, 9).

Genetic Determinism of Coiling Direction.—The present sample set should be expanded before coiling rules within the *G. truncatulinoides* species complex are asserted. Nevertheless our molecular data suggest a basic, genetic influence on the coiling direction of the test. First, sp. 1 coils left at the same latitudes where sp. 2 coils right (Fig. 9). Second, the right-coiled South Atlantic and left-coiled North Atlantic specimens of sp. 2 correspond to distinct genetic clusters (Fig. 5). Thus, we detected correlations between coiling direction and genetic clustering at species and population levels. This further suggests that the coiling provinces of the *G. truncatulinoides* complex may result from the simple reproductive isolation of populations, which may explain the uncertainty and divergence of opinions on the factors controlling the complicated coiling-direction patterns observed in *G. truncatulinoides* (Kennett 1976). Note that obvious ecological differences between left- and right-coiled specimens recognized in the North Atlantic (Hemleben et al. 1985; Lohmann and Schweitzer 1990) strongly argue for at least two different species or populations in the Northern Hemisphere too.

Mode of Speciation in Planktic Foraminifera.—Our genetic analysis, with the timing of speciation provided by the molecular clock and the fossil record, together with the information on morphological and ecological differentiations associated with the genetic events, allows us to question the evolutionary processes leading to the establishment of the *G. truncatulinoides* complex of species.

Several hypotheses compete concerning the nature of the processes involved in genetic isolation in very highly dispersive organisms like planktic foraminifera. Speciation could have been induced entirely by genetic mechanisms, like gamete incompatibility or a complex mating system, as it has been observed in other groups of highly dispersive oceanic organisms (Palumbi 1992). In such a case, the morphological differentiation may be simply the consequence of a drift occurring after genetic isolation.

However, the recent species diversification and the different environmental preferences of the species suggest that adaptive advantages might have favored genomic isolation, possibly as an evolutionary response to colonizing new habitats. Hence, it is possible that morphological differentiations have been

driven by direct adaptive advantages related to test size and shape, like the sinking resistance to maintain the level in the nutrient-rich upper waters (Healy-Williams 1985; Wei 1994) for the small and lenticular frontal and subpolar species, and the size-related differences in the number of gametes (Lohmann 1992) for the larger subtropical species.

Moreover, different lines of evidences suggest that adaptive speciation has been linked to a heterochronic process. First, both our plankton samples (Fig. 10) and sediment analyses (Hills 1988; Lohmann and Malmgren 1983; Mulitza et al. 1997) indicate a latitudinal size variation within the *G. truncatulinoides* complex. Second, we detected an allometric relationship between size and shape for the subtropical species (sp. 3–sp. 4). Sections cut through individual tests also demonstrate this change from a small biconvex juvenile to a highly conical adult morphology in subtropical *G. truncatulinoides* (Postuma 1971). Thus an obvious morphological convergence exists between juvenile, subtropical *G. truncatulinoides* and mature adults of the subpolar morphs, which is also known from sediments (Takayanagi et al. 1968; Pharr 1983; Healy-Williams et al. 1985; Lohmann 1992). Small subpolar specimens seem to correspond to mature adults with retention of ancestral juvenile characters of the subtropical stem species.

Hence we propose that highly variable environments such as hydrographic frontal zones might favor more precocious (and frequent) reproduction in planktic foraminifera, contributing to establish a sharp barrier to reproduction by isolating the gametogenesis events in the new emerging species. This progenesis hypothesis is supported by observations that timing and even mode of reproduction may shift very rapidly in foraminifera under stressed conditions. A few cases of adult retention of an ancestral juvenile character complex have been detected in fossil planktic foraminifera (Wei 1994; Kelly et al. 1999). Our data suggest these cases may have been largely underestimated—owing to the selection of a narrow size range in many morphological analyses—and that speciation may be currently associated with heterochronic processes and niche adaptation in planktic foraminifera.

Conclusions

The important underestimation of biodiversity detected here in one of the most studied planktic foraminifers has been observed within the six other morphospecies genetically analyzed so far (Huber et al. 1997; Darling et al. 1999, 2000; de Vargas et al. 1999, in press). Each actually represents a cluster of three to five distinct but related genetic species, whose slight morphological differences have been either overlooked or attributed to ecophenotypy in traditional morphological analyses. Clearly, speciation does not necessary imply significant morphological change in planktic foraminifera and species concepts need to be reconsidered from a biological point of view.

The limited molecular studies on other holoplanktic organisms—from bacteria (Giovannoni et al. 1990; DeLong et al. 1994) and unicellular phytoplankton (Ferris and Palenik 1998; Fuhrman and Campbell 1998; Moore et al. 1998) to vertebrates (Miya and Nishida 1997)—have shown that cryptic diversity is a common phenomenon in the open ocean. The pelagic domain, an extremely dispersive and relatively homogeneous environment, is manifestly biologically more structured than previously assumed.

In addition, the revealed pelagic diversity often corresponds to physiological evolution (Moore et al. 1998) and adaptation to specific water masses or depths (Ferris and Palenik 1998). Apparently, in all planktic foraminiferal lineages that have been phylogeographically analyzed so far—*G. truncatulinoides, Orbulina universa* (de Vargas et al. 1999), or *Globigerinella siphonifera* (de Vargas et al. in press)—the various genetic species within a morphologic entity seem to have adapted to different hydrographic conditions. The stability of the water column and subsequent productivity have obviously played a key role in their adaptive radiation (de Vargas et al. 1999) (Fig. 7). Our study further suggests that simple heterochronic reproductive behaviors associated with niche adaptation may be a common mode of speciation in planktic foraminifera and may explain the high morphologi-

cal coherence conserved between genetically related species.

Thus, many planktic foraminiferal species may have much narrower geographic ranges and ecological requirements than has been suspected, and very slight morphological differences may distinguish related species adapted to significantly different environments. This conclusion drastically changes our view on evolutionary processes, biogeography, and ecology in planktic foraminifera, and may question some of the stratigraphic or paleoecologic inferences based on the classical morphological concepts of species. In the case of *G. truncatulinoides*, for instance, the morphological changes recorded over the last 700 k.y. in the sediment core CHAIN 115-88PC (Lohmann and Malmgren 1983; Lohmann 1992), located close to our station AMT-23 (Fig. 7), should be interpreted as evolution in the (sp. 3–sp. 4) ancestor, rather than the ecophenotypic expression of paleoceanographic changes, in the new multispecies context.

Finally, our results show the potential of combined DNA and morphometric analyses for increasing the resolving power of the foraminiferal fossil record. DNA sequences used as a taxonomic tool and time machine allowed us to distinguish the different species and establish their phylogeny, estimate their separation time and hydrographic preferences, and detect morphological characters correlated to genetic differentiation. Despite the blurring in the fossil record due to changes in the position of the water masses through time (seasonal and long-term), lateral transport of the sinking tests, slow sedimentation rate, and sediment reworking, our data strikingly mirror, in both space and time, the previous observations of the Pleistocene and Recent *G. truncatulinoides* sediment record. The challenge is now to describe further the genetic species of planktic foraminifera, their biogeographic ranges, and their ecological requirements, and to learn to recognize the characters in their tests (ultrastructure, chemistry or isotopic content) that will enable us to distinguish them. This may allow us to dramatically improve the resolution of climate and stratigraphic proxies by developing more precise planktonic foraminiferal probes for applied work in the future.

Acknowledgments

We thank D. Schmidt for help during morphometric measurements and helpful discussions, and J. Fahrni for sequencing assistance. We are indebted to R. Norris, R. Peck, L. Zaninetti, W. Berggren, L. Excoffier, and Lobi for fruitful discussions, and to D. B. Robbins and J. Aiken, and C. and J. Febvre-Chevalier, who allowed the specimens collection on the AMT cruise and in the Mediterranean Sea, respectively. We would like to acknowledge the work of the officers, crew, and scientists onboard the RRS *James Clark Ross.* We gratefully acknowledge B. T. Huber and D. Lazarus for their helpful criticism of the manuscript. This is publication 45 of the AMT program. This research was supported by the Swiss National Foundation Grant 31-49513.96 (J. P.) and 2053-053676.98 (H. H.).

Literature Cited

Bolli, H. M., and J. B. Saunders. Late Middle Eocene to Recent planktonic foraminiferal biostratigraphy. Pp. 144–262 *in* H. M. Bolli, J. B. Saunders, and K. Perch-Nielsen, eds. Plankton stratigraphy. Cambridge University Press, Cambridge.

Crampton, J. S. 1995. Elliptic Fourier shape analysis of fossil bivalves: some practical considerations. Lethaia 28:179–186.

Darling, K., C. M. Wade, D. Kroon, A. J. Leigh Brown, and J. Bijma. 1999. The diversity and distribution of modern planktic foraminiferal small subunit ribosomal RNA genotypes and their potential as tracers of present and past ocean circulations. Paleoceanography 14:3–12.

Darling, K., C. M. Wade, I. A. Stewart, D. Kroon, R. Dingle, and A. J. Leigh Brown. 2000. Molecular evidence for genetic mixing of Arctic and Antarctic subpolar populations of planktonic foraminifers. Nature 405:43–47.

DeLong E. F., K. Y. Wu, B. B. Prézelin, and R. V. M. Jovine. 1994. High abundance of Archaea in Antarctic marine picoplankton. Nature 371:695–697.

Deuser, W. G., E. H. Ross, C. Hemleben, and M. Spindler. 1981. Seasonal changes in species composition, number, mass, size, and isotopic composition of planktonic foraminifera settling into the deep Sargasso Sea. Palaeogeography, Palaeoclimatology, Palaeoecology 33:103–127.

de Vargas, C., and J. Pawlowski. 1998. Molecular versus taxonomic rates of evolution in planktonic foraminifera. Molecular Phylogenetics and Evolution 9:463–469.

de Vargas, C., L. Zaninetti, H. Hilbrecht, and J. Pawlowski. 1997. Phylogeny and rates of molecular evolution of planktonic foraminifera: SSU rDNA sequences compared to the fossil record. Journal of Molecular Evolution 45:285–294.

de Vargas, C., R. Norris, L. Zaninetti, S. W. Gibb, and J. Pawlowski. 1999. Molecular evidence of cryptic speciation in planktonic foraminifers and their relation to oceanic provinces. Proceedings of the National Academy of Sciences USA 96: 2864–2868.

de Vargas, E., M. Bonzon, N. Rees, J. Pawlowski, and L. Zani-

netti. In press. A molecular approach to biodeversity and biogeography in the planktonic foraminifera*Globigerinella siphonifera* (d'Orbigny). Marine Micropaleontology.

Ehrlich, R., and B. Weinberg. 1970. An exact method for characterization of grain shape. Journal of Sedimentary Petrology 40:205–212.

Fairbanks, R. G., and P. H. Wiebe. 1980. Foraminifera and chlorophyll maximum: vertical distribution, seasonal succession, and paleoceanographic significance. Science 209:1524–1526.

Ferris, M. J., and B. Palenik. 1998. Niche adaptation in ocean cyanobacteria. Nature 396:226–228.

Fuhrman, J. A., and L. Campbell. 1998. Microbial biodiversity. Nature 393:410–411.

Galtier, N., and M. Gouy. 1996. SEAVIEW and PHYLO_WIN: two graphic tools for sequence alignment and molecular phylogeny. Computer Applications in the Biosciences 12:543–548.

Giovannoni, S. J., T. B. Britschgi, C. L. Moyer, and K. G. Field. 1990. Genetic diversity in Sargasso Sea bacterioplankton. Nature 344:60–63.

Healy-Williams, N. 1983. Fourier shape analysis of *Globorotalia truncatulinoides* from late Quaternary sediments in the southern Indian Ocean. Marine Micropaleontology 8:1–15.

Healy-Williams, N., and D. F. Williams. 1981. Fourier analysis of test shape of planktonic foraminifera. Nature 289:485–487.

Healy-Williams, N., R. Ehrlich, and D. F. Williams. 1985. Morphometric and stable isotopic evidence for subpopulations of *Globorotalia truncatulinoides.* Journal of Foraminiferal Research 15:242–253.

Hemleben, C., M. Spindler, I. Breitinger, and W. G. Deuser. 1985. Field and laboratory studies on the ontogeny and ecology of some globorotaliid species from the Sargasso Sea off Bermuda. Journal of Foraminiferal Research 15:254–272.

Hemleben, C., M. Spindler, and O. R. Anderson. 1989. Modern planktonic foraminifera. Springer, New-York.

Hills, S. J. 1988. The analysis of microfossil shape: experiments using planktonic foraminifera. Ph.D. dissertation. University of California, San Diego.

Hills, S. J., and H. R. Thierstein. 1989. Plio-Pleistocene calcareous plankton biochronology. Marine Micropaleontology 14: 67–69.

Holzmann, M., W. Piller, and J. Pawlowski. 1996. Sequence variations in the Large-SubUnit RNA gene of *Ammonia* (Foraminifera, Protozoa) and their evolutionary implications. Journal of Molecular Evolution 43:145–151.

Hooker, S. B., N. W. Rees, and J. Aiken. In press. An objective methodology for identifying oceanic provinces. Progress in Oceanography.

Huber, B. T., J. Bijma, and K. Darling. 1997. Cryptic speciation in the living planktonic foraminifer *Globigerinella siphonifera* (d'Orbigny). Paleobiology 23:33–62.

Kelly, D. C, A. J. Arnold, and W. C. Parker. 1999. The influence of heterochrony on the stratigraphic occurrence of *Morozovella ungulata.* Journal of Foraminiferal Research 29:58–68.

Kennett, J. P. 1968. *Globorotalia truncatulinoides* as a paleo-oceanographic index. Science 159:1461–1463.

———. 1970. Pleistocene paleoclimates and foraminiferal biostratigraphy in subantarctic deep-sea cores. Deep-Sea Research 17:125–140.

———. 1976. Phenotypic variation in some Recent and Late Cenozoic planktonic foraminifera. Pp. 1–60 *in* R. H. Hedley and C. G. Adams, eds. Foraminifera, Vol. 2, Academic Press, London.

Kennett, J. P., and M. S. Srinivasan. 1983. An atlas of Neogene planktonic foraminifera: phylogenetic approach. Hutchinson and Ross, Stroudsburg, Penn.

Larsen, N., G. J. Olsen, B. L. Maidak, M. J. McCaughey, R. Overbeek, T. J. Macke, T. L. Marsh, and C. R. Woese. 1993. The ribosomal database project. Nucleic Acids Research 21:3021–3023.

Lazarus, D., H. Hilbrecht, C. Spencer-Cervato, and H. Thierstein. 1995. Sympatric speciation and phyletic change in *Globorotalia truncatulinoides.* Paleobiology 21:26–51.

Lohmann, G. P. 1992. Increasing seasonal upwelling in the subtropical South Atlantic over the past 700,000 yrs: evidence from deep-living planktonic foraminifera. Marine Micropaleontology 19:1–12.

Lohmann, G. P., and B. A. Malmgren. 1983. Equatorward migration of *Globorotalia truncatulinoides* ecophenotypes through the Late Pleistocene: gradual evolution or ocean change? Paleobiology 9:414–421.

Lohmann, G. P., and P. N. Schweitzer. 1990. *Globorotalia truncatulinoides*: growth and chemistry as probes of the past thermocline. 1. Shell size. Paleoceanography 5:55–75.

Martinez, J. I. 1997. Decreasing influence of Subantarctic Mode Water north of the Tasman Front over the past 150 ky. Palaeogeography, Palaeoclimatology, Palaeoecology 131:355–364.

Miya, M., and M. Nishida. 1997. Speciation in the open ocean. Nature 389:803–804.

Moore, L. R., G. Rocap, and S. W. Chisholm. 1998. Physiology and molecular phylogeny of coexisting *Prochlorococcus* ecotypes. Nature 393:464–467.

Mulitza, S., A. Dürkoop, H. Walter, G. Wefer, and H. S. Niebler. 1997. Planktonic foraminifera as recorders of past surface-water stratification. Geology 25:335–338.

Norris, R. D., R. M. Corfield, and J. E. Cartlidge. 1994. Evolutionary ecology of *Globorotalia* (*Globoconella*) (planktic foraminifera). Marine Micropaleontology 23:121–145.

Olsen, G. J., H. Matsuda, R. Hagstrom, and R. Overbeek. 1994. FastDNAml: a tool for construction of phylogenetic trees of DNA sequences using maximum likelihood. Computer Applications in the Biosciences 10:41–48.

Palumbi, S. R. 1992. Marine speciation on a small planet. Trends in Ecology and Evolution 7:114–118.

Pawlowski, J., I. Bolivar, J. Fahrni, C. de Vargas, M. Gouy, and L. Zaninetti. 1997. Extreme differences in rates of molecular evolution of foraminifera revealed by comparison of ribosomal DNA sequences and the fossil record. Molecular Biology and Evolution 14:498–505.

Perrière G., and M. Gouy. 1996. WWW-Query: an on-line retrieval system for biological sequence banks. Biochimie 78: 364–369.

Pharr, R. B. 1983. Examination of the late Quaternary paleobiology of *Globorotalia truncatulinoides* using Fourier shape analysis. Ph.D. dissertation. University of South Carolina, Columbia.

Pharr, R. B., Jr., and D. F. Williams. 1987. Shape changes in *Globorotalia truncatulinoides* as a function of ontogeny and paleobiogeography in the southern ocean. Marine Micropaleontology 12:343–355.

Postuma, J. A. 1971. Manual of planktonic foraminifera. Elsevier, Amsterdam.

Renaud, S., and C. Girard. 1999. Strategies of survival during extreme environmental perturbations: evolution of conodonts in response to the Kellwasser crisis (Upper Devonian). Palaeogeography, Palaeoclimatology, Palaeoecology 146:19–32.

Renaud, S., J. Michaux, J.-J. Jaeger, and J.-C. Auffray. 1996. Fourier analysis applied to *Stephanomys* (Rodentia, Muridae) molars: nonprogressive evolutionary pattern in a gradual lineage. Paleobiology 22:255–265.

Renaud, S., M. Benammi, and J.-J. Jaeger. 1999a. Morphological evolution of the murine rodent *Paraethomys* in response to climatic variations (Mio-Pliocene of North Africa). Paleobiology 25:369–382.

Renaud, S., J. Michaux, P. Mein, J.-P. Aguilar, and J.-C. Auffray. 1999b. Patterns of size and shape differentiation during the

evolutionary radiation of the European Miocene murine rodents. Lethaia 32:61–71.

Robins, D. B., and J. Aiken. 1996. The Atlantic Meridional Transect: an oceanographic research programme to investigate physical, chemical, biological and optical variables of the Atlantic Ocean. Underwater Technology 21:8–14.

Rohlf, F. J., and J. W. Archie. 1984. A comparison of Fourier methods for the description of wing shape in mosquitoes (Diptera: Culicidae). Systematic Zoology 33:302–317.

Saitou, N., and M. Nei. 1987. The neighbor-joining method: a new method for reconstructing phylogenetic trees. Molecular Biology and Evolution 4:406–425.

Spencer-Cervato, C., and H. R. Thierstein. 1997. First appearance of *Globorotalia truncatulinoides*: cladogenesis and immigration. Marine Micropaleontology 30:267–291.

Stanley, S. M., K. L. Wetmore, and J. P. Kennett. 1988. Macroevolutionary differences between the two major clades of Neogene planktonic foraminifera. Paleobiology 14:235–249.

Tajima, F., and M. Nei. 1984. Estimation of evolutionary distance for reconstructing molecular phylogenetic trees. Molecular Biology and Evolution 18:278–286.

Takayanagi, Y., N. Niitsuma, and T. Sakai. 1968. Wall microstructure of *Globorotalia truncatulinoides* d'Orbigny. Science report of Tohoku University, 2d series (Geology) 40:141–170.

Thiede, J. 1971. Variations in coiling ratios of Holocene planktonic foraminifera. Deep-Sea Research 18:823–831.

Wei, K. 1994. Allometric heterochrony in the Pliocene-Pleistocene planktic foraminiferal clade *Globoconella*. Paleobiology 20:66–84.

Willson, H. R., and N. W. Rees. In press. Use of in situ and satellite imagery to interpret mesoscale features in the Brazil-Falkland current confluence zone. Progress in Oceanography.